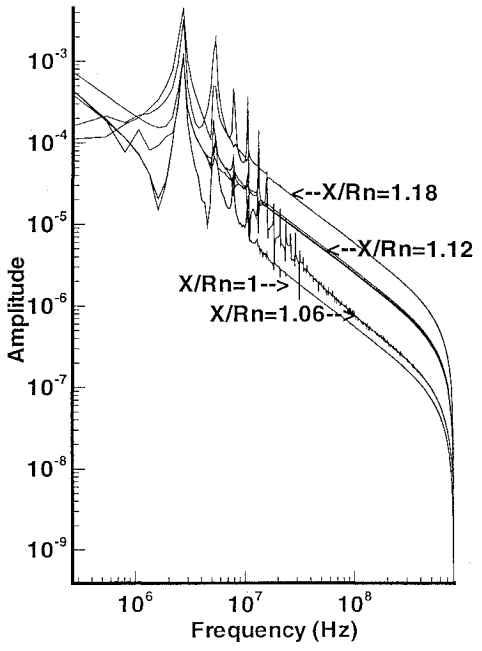

Fig. 5 Temporal frequency spectrum of water mass fraction for Mach 6.46 for 197 × 152 grid size.

are also shown. Thus, refining the grid from 131 × 101 to 197 × 152 has not significantly changed the frequency and, therefore, the oscillations in the reaction front are physical. Experimental fundamental frequency for the Mach 6.46 case is not available.

Conclusions

A numerical study is carried out to investigate the shock-induced combustion in premixed hydrogen-air mixture. The calculations have been carried out for Mach 5.11 and 6.46. The Mach 5.11 case was found to be unsteady with periodic oscillations. The frequency of oscillations was calculated and was found to be in good agreement with the experimentally observed frequency. The Mach 6.46 case was found to be of a very high frequency and very low-amplitude phenomena. Thus it can be considered as macroscopically stable. This supports the existing view that it is possible to stabilize the shock-induced combustion phenomena with sufficient level of overdrive.

References

[1]Lehr, H. F., "Experiments on Shock-Induced Combustion," *Acta Astronautica*, Vol. 17, Sept. 1972, pp. 586–589.

[2]Anonymous., Rapport-Bericht CO 7/73, Institut Franco-Allenmand De Recherches De Saint-Louis, Kolloquium Uber Gasdetonationen, obgehalten im ISL am 22.10.1973, ISL-Beitrage.

[3]Ahuja, J. K., and Tiwari, S. N., "Investigation of Hypersonic Shock-Induced Combustion in a Hydrogen-Air System," AIAA Paper 92-0339, Jan. 1992.

[4]Ahuja, J. K., and Tiwari, S. N., "Numerical Simulation of Shock-Induced Combustion in a Superdetonative Hydrogen-Air System," AIAA Paper 93-0242, Jan. 1993.

[5]Singh, D. J., Ahuja, J. K., and Carpenter, M. H., "Numerical Simulations of Shock-Induced Combustion/Detonation," *Computing Systems in Engineering*, Vol. 3, 1992, pp. 201–215.

[6]Wilson, G. J., and MacCormack, R. W., "Modelling Supersonic Combustion Using a Fully-Implicit Numerical Method," *AIAA Journal*, Vol. 30, No. 4, 1992, pp. 1008–1015.

[7]Sussman, M. A., "Source Term Evaluation for Combustion Modelling," AIAA Paper 93-0239, Jan. 1993.

[8]Wilson, G. J., and Sussman, M. A., "Computation of Unsteady Shock-Induced Combustion Using Logarithmic Species Conservation Equations," *AIAA Journal*, Vol. 31, 1993, pp. 294–301.

[9]Matsuo, A., and Fujiwara, T., "Numerical Simulations of Shock-Induced Combustion around an Axisymmetric Blunt Body," AIAA Paper 91-1414, June 1991.

[10]Matsuo, A., and Fujiwara, T., "Numerical Investigation of Oscillatory Instability in Shock-Induced Combustion around a Blunt Body," *AIAA Journal*, Vol. 31, 1993, pp. 1835–1841.

[11]Matsuo, A., Fujiwara, T., and Fujii, K., "Flow Features of Shock-Induced Combustion around Projectiles Travelling at Hypervelocities," AIAA Paper 93-0451, Jan. 1993.

[12]Ahuja, J. K., and Tiwari, S. N., "A Parametric Study of Shock-Induced Combustion in a Hydrogen-Air System," AIAA Paper 94-0674, Jan. 1994.

[13]McVey, J. B., and Toong, T. Y., "Mechanism of Instabilities of Exothermic Hypersonic Blunt-Body Flows," *Combustion Science and Technology*, Vol. 3, 1971, pp. 63–76.

[14]Jachimowski, C. J., "An Analytical Study of the Hydrogen-Air Reaction Mechanism with Application to Scramjet Combustion," NASA TP-2791, 1988.

[15]Drummond, J. P., Rogers, R. C., and Hussaini, M. Y., "A Detailed Numerical Model of a Supersonic Reacting Mixing Layer," AIAA Paper 86-1427, June 1986.

[16]MacCormack, R. W., "The Effect of Viscosity in Hypervelocity Impact Cratering," AIAA Paper 69-354, April–May 1969.

Observations on Using Experimental Data as Boundary Conditions for Computations

Paul D. Orkwis,* Chung-Jen Tam,† and Peter J. Disimile‡
University of Cincinnati, Cincinnati, Ohio 45221

Introduction

MANY computational efforts have been undertaken to simulate phenomena that have been studied experimentally. Numerous examples of this are found in the recent work on open cavity flows by Hankey and Shang,[1] Rizzetta,[2] Baysal et al.,[3] and others. These computations attempted to match the conditions of an experiment by employing the same nondimensional flowfield parameters, such as Mach and Reynolds numbers, and identical geometries. However, without intimate knowledge of the experimental procedures and apparatus it is impossible to match all of the boundary conditions for these flowfields. This knowledge includes the data collection procedures, the construction of the model, the proximity of the wind-tunnel walls, and the conditions outside of the test section. Researchers typically either ignore these details or assume an idealized configuration. This Note describes the procedures employed by the authors to determine computational boundary conditions from an experimental supersonic open cavity flowfield study and the observations made during this process.

Observations

An experimental and computational research program[4] has been undertaken to study the flow physics of supersonic open cavity flowfields such as those encountered by stealthy fighter, attack, and bomber aircraft. This effort requires a synergistic approach to acquire valid field and surface data because neither experimental nor computational methodologies are capable of efficiently producing both. Acquired experimental data include time-averaged surface pressures, time histories of surface pressures, upstream boundary-layer streamwise velocities, and qualitative surface streaking using shear stress sensitive liquid crystals. Computational data include time histories of all field properties. These computational data can then be time averaged and compared with the surface data obtained

Presented as Paper 94-0589 at the AIAA 32nd Aerospace Sciences Meeting, Reno, NV, Jan. 10–13, 1994; received July 13, 1994; revision received Sept. 12, 1994; accepted for publication Sept. 30, 1994.

*Assistant Professor, Department of Aerospace Engineering and Engineering Mechanics. Member AIAA.

†Research Assistant. Member AIAA.

‡Associate Professor, Department of Aerospace Engineering and Engineering Mechanics. Member AIAA.

in the experiments to assess the accuracy of the computations and to validate the turbulence modeling assumptions. This approach then produces valid qualitative and quantitative field and surface property information that can be used to uncover the dynamic mechanisms that drive open cavity flowfields.

Two-dimensional flows were simulated by employing a cavity with a width-to-length ratio (W/L) of approximately 12 and a length-to-depth ratio (L/D) of 2, as shown in Fig. 1. The wind-tunnel freestream conditions for these tests were Mach number $M = 2$ and unit Reynolds number $Re/L = 37.7 \times 10^6$/m.

It was initially assumed that the experimental data would be ideal for the purpose of determining valid upstream boundary conditions for the cavity computations. Therefore, pitot pressure surveys were conducted (several times to assure repeatability) 1.94 cm upstream of the cavity separation lip to determine the upstream velocity profile shown in Fig. 2. These data were then fitted to a power law profile with an exponent of 8.4, which allowed velocities to be found at all computational grid points. A temperature profile was then found by employing the turbulent Crocco-Busemann relation

$$T = T_w + (T_{aw} - T_w)\frac{u}{U_\infty} - r\frac{u^2}{2C_p} \tag{1}$$

with the experimentally determined wall temperature of 239 K. It should be noted that in Eq. (1) w corresponds to wall conditions, aw to adiabatic wall conditions, and r to the recovery factor, i.e., $P_r^{\frac{1}{3}}$, where P_r is the Prandtl number. The remaining variables, density and total energy, were then found by assuming a perfect gas and zero normal velocity.

However, the zero normal velocity assumption proved to be detrimental to the computational solution, as can be seen in the computed time-averaged cavity surface pressures shown in Fig. 3 for two different inflow conditions. In case A the power law profile discussed earlier was used as the inflow velocity distribution, and in case B a computationally generated flat plate solution was employed that matched the experimental momentum thickness (shown in Fig. 2). Both sets of results were obtained using the standard Baldwin-Lomax turbulence model and a computational grid with a minimum y^+ of 44. Results from five cavity characteristic times, defined as L/U_∞ (L is the cavity length) were used to obtain the averages. The results compared quite well with the experimental data when the computational inflow condition was used, but the results

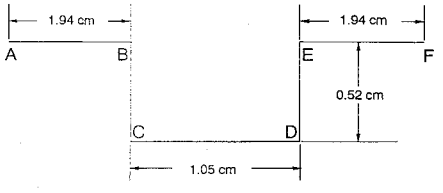

Fig. 1 Two-dimensional cavity schematic.

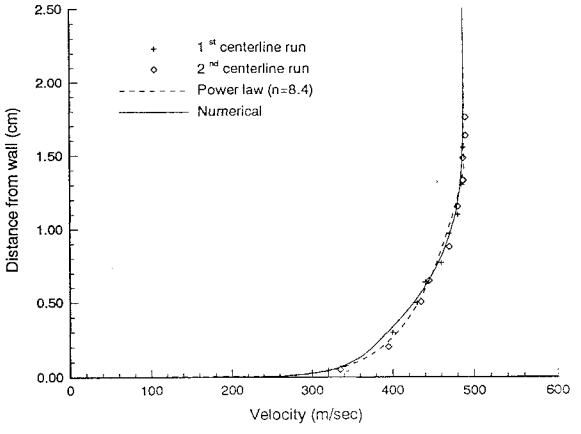

Fig. 2 Comparison of experimental and computational velocity profiles.

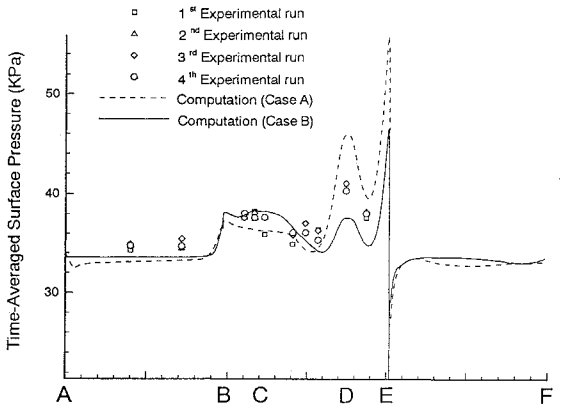

Fig. 3 Comparison of experimental and computational surface pressures.

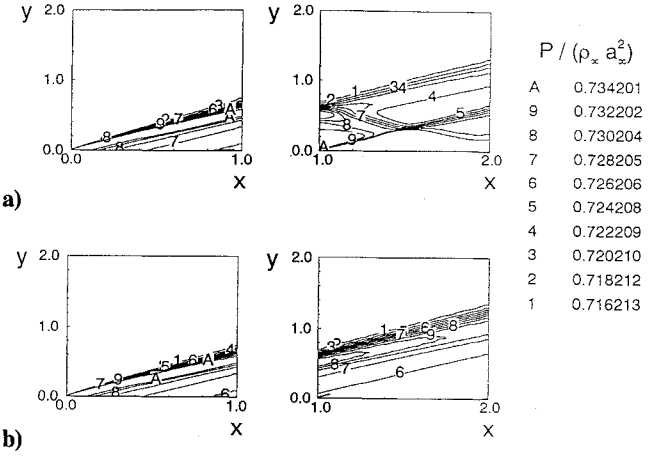

Fig. 4 Pressure contours of consecutive flat plate calculations; a) zero normal velocity and b) actual velocity.

differed by as much as 11% when the experimental profile with zero normal velocity was employed.

The differences in the results were caused by the assumption of zero normal velocity. This was proven by a numerical study that produced the pressure contour results shown in Fig. 4, in which upstream boundary conditions derived from an initial flat plate solution were used to extend the flat plate solution further downstream. The flow properties from the next to last grid line of the initial flat plate were used as the upstream boundary condition for the flat plate extension. Case A employed a profile with zero normal velocity and case B used the full velocity profile. The left contours for both cases are from the same initial flat plate solution. The contours clearly illustrate the formation of spurious shock and expansion waves as a result of the $v = 0$ assumption. Similar contours are produced for the other solution variables and are not shown.

It should be noted that the previous configuration is not the same as that used in the cavity flow computations. In that case a much longer plate was required to match the experimental momentum thickness; consequently, the bow shock wave propagated out of the solution domain. The shorter plate was employed in the previous computation because it provides a much clearer example of the errors inherent in neglecting small velocity components. In addition, the initial drop in surface pressure of the cavity model (see Fig. 3) clearly demonstrates similar trends. These discrepancies might be lessened if the point of boundary condition application was moved further upstream, since the flow would have a greater distance to adjust to the erroneous velocity specification. The results show that care must be taken to insure complete specification of boundary conditions if experimental data are to be employed.

Summary

This effort has shown that a complete description of the flowfield properties is required to pose accurately boundary conditions for a

computational simulation that is to match experimental data. Inclusion of the experimental normal velocity was shown to be vital for the derivation of correct computational boundary conditions. Streamwise velocity profiles determined from pitot probe measurements were found to be insufficient for this purpose; hence, techniques capable of determining both streamwise and normal velocity must be employed.

Acknowledgments

The authors wish to thank Dr. Leonidas Sakell and the Air Force Office of Scientific Research for their generous support through Grant F49620-93-1-0081. This work was supported in part by a grant of HPC time from the Department of Defence HPC Shared Resource Center, U.S. Army Corps of Engineers—Waterways Experiment Station C916/16512 Supercomputer.

References

[1]Hankey, W. L., and Shang, J. S., "Analysis of Pressure Oscillations in an Open Cavity," *AIAA Journal*, Vol. 18, No. 8, 1980, pp. 892–898.

[2]Rizzetta, D. P., "Numerical Simulation of Supersonic Flows over a Three-Dimensional Cavity," *AIAA Journal*, Vol. 26, No. 7, 1988, pp. 799–807.

[3]Baysal, O., Fouladi, K., Leung, R. W., and Sheftic, J. S., "Interference Flows Past Cylinder-Fin-Sting-Cavity Assemblies," *Journal of Aircraft*, Vol. 29, No. 2, 1992, pp. 194–202.

[4]Dusing, D. W., Fox, C. W., Tam, C.-J., Orkwis, P. D., and Disimile, P. J., "An Experimental and Computational Study of Unsteady Supersonic 2-D Open Cavity Flow Physics," AIAA Paper 94-0589, Jan. 1994.

Scaling of Incipient Separation in Supersonic/Transonic Speed Laminar Flows

George R. Inger*
Iowa State University, Ames, Iowa 50010

Nomenclature

C = Chapman-Rubesin parameter, $\mu T_\infty/\mu_\infty T$
L = reference length (see Fig. 1)
M = Mach number
p = static pressure
Re_L = Reynolds number $\cong \varepsilon^{-8}$, $\rho_\infty U_\infty L/\mu_\infty$
T = absolute static temperature
U_∞ = freestream velocity at edge of incoming boundary layer
u, v = velocity components in x, y directions, respectively
x, y = streamwise and normal coordinates, respectively
β = $(M_\infty^2 - 1)^{\frac{1}{2}}$
δ^* = displacement thickness variable
θ = flow deflection angle
μ = coefficient of viscosity, $\equiv \rho\nu$
ρ = density
χ = viscous interaction parameter, $M_\infty^3 Re_L^{-\frac{1}{2}}$
ω = viscosity temperature-dependence exponent ($\mu \sim T^\omega$)

Subscripts

ADIAB = adiabatic wall conditions
$i.s.$ = incipient separation
REF = based on reference temperature
w = wall surface conditions

Superscript

$(\hat{})$ = nondimensional variables from triple-deck theory

Presented in part as AIAA Paper 93-3435 at the AIAA 11th Applied Aerodynamics Conference, Monterey, CA, Aug. 9–13, 1993; received Feb. 26, 1994; revision received Aug. 2, 1994; accepted for publication Aug. 20, 1994.

*Professor, Department of Aerospace Engineering and Engineering Mechanics. Associate Fellow AIAA.

Introduction

INTERACTIONS between oblique shock waves and boundary layers must be understood to predict the performance of aerodynamic devices such as flaps, spoilers, and inlets. These involve strong viscous/inviscid interaction flow with a large local adverse pressure gradient that often provokes boundary-layer separation. The prediction of the onset of such separation and the delineation of the underlying scaling laws that govern it continue to be important in aerodynamic studies of high speed aircraft and missiles, these vehicles operate and are tested over a wide range of Mach and Reynolds numbers. This paper re-examines the fundamental similitude rules pertaining to the laminar (high-altitude) flight regime of supersonic vehicles, with the goal of establishing a single unified scaling law for both supersonic and moderately hypersonic Mach numbers.

We consider two-dimensional steady laminar flow of an ideal gas that undergoes incipient separation in the strong interaction region associated with either an impinging shock or a compression corner (Fig. 1). This event is characterized by a critical value of the forcing function (e.g., a deflection angle or nondimensional shock pressure

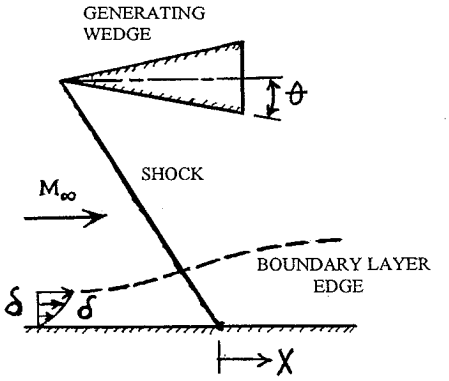

a) Impinging shock

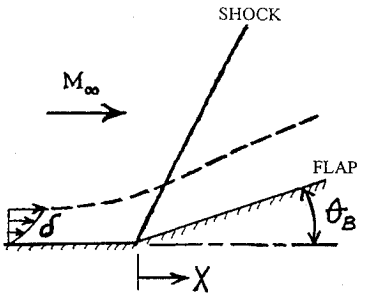

b) Compression corner

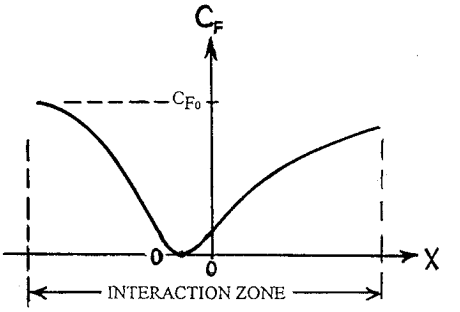

c) Definition of incipient separation

Fig. 1 Regions of local shock/boundary layer interaction.